Niger. J. Physiol. Sci. 39 (December 2024): 267 – 276
www.njps.physiologicalsociety.com

Niger. J. Physiol. Sci.

Full length Research Article

Ursolic Acid Ameliorates Vascular Oxidative Stress and Upregulates Endothelial Nitric Oxide Synthase Gene in Male Wistar Rats with High-carbohydrate High-fat Diet-induced Metabolic Syndrome

***Omodara, O.O.[1], Kawu, M.U.[2], Bako, I.G.[3], Isa, A.S.[3], Mhya, H.D.[4], Ali, Z.[1].**

Departments of [1]Human Physiology and [4]Medical Biochemistry, Faculty of Basic Medical Sciences, College of Medical Sciences, Abubakar Tafawa Balewa University, Bauchi, Nigeria.

[2]Department of Veterinary Physiology, Faculty of Veterinary Medicine, Ahmadu Bello University, Zaria, Nigeria

[3]Department of Human Physiology, Faculty of Basic Medical Sciences, College of Medical Sciences, Ahmadu Bello University, Zaria, Nigeria.

Summary: The development of cardiovascular diseases and type 2 diabetes is preceded by the risk factors of metabolic syndrome (MS) which are often induced by high-carbohydrate high-fat diet (HCHFD) together with sedentary lifestyle. These risk factors are associated with vascular dysfunction. Our previous study has shown that ursolic acid (UA) prevents the development of these risk factors of MS induced by HCHFD, but the potential mechanism involved in the amelioration of vascular oxidative stress induced by HCHFD has not been explained. This study investigated the mechanism by which dietary UA supplementation improves vascular oxidative stress in male Wistar rats fed a HCHFD. Twenty (20) male Wistar rats were randomly divided into 4 groups (n =5): 1- normal diet (ND) + distilled water (DW); 2 – ND+UA; 3 – HCHFD+DW; 4 – HCHFD+UA. HCHFD was formulated in-house. The animals were fed their respective diets daily for 20 weeks. The drinking water of animals fed a HCHFD was augmented with 20% fructose. 250 mg/kg body weight of ursolic acid was administered orally to UA-treated groups for the last 8 weeks of the study. Body mass index (BMI) and abdominal circumference were evaluated; serum insulin and nitric oxide were assessed by using enzyme-linked immunosorbent assay kits; and insulin resistance was determined using the homeostatic model assessment for insulin resistance (HOMA-IR). Aortic antioxidant enzymes and reactive oxygen species were evaluated. Aorta and adipose tissues' endothelial nitric oxide synthase (eNOS) was evaluated using real-time polymerase chain reaction technique. There was a significantly ($P<0.05$) lowered BMI percentage increase in the HCHFD+UA-fed animals compared to the HCHFD+DW-fed animals. In the HCHFD+UA-fed animals, serum insulin and HOMA-IR were significantly ($P<0.05$) decreased compared to the HCHFD+DW-fed animals. Serum nitric oxide was significantly ($P<0.05$) increased in HCHFD+UA-fed animals compared to the HCHFD+DW-fed animals. In HCHFD+UA-fed animals, aorta superoxide dismutase, catalase and glutathione were significantly ($P<0.05$) increased, compared to the HCHFD+DW-fed animals. Aorta reactive oxygen species was significantly ($P<0.05$) decreased in HCHFD+UA-fed animals compared to the HCHFD+DW-fed animals. Both aorta and adipose tissue eNOS mRNA level was significantly ($P<0.05$) more expressed in the HCHFD+UA-fed animals compared to the HCHFD+DW-fed animals. Findings from this study showed that ursolic acid supplementation ameliorates vascular oxidative stress and upregulates eNOS gene in male Wistar rats with high-carbohydrate high-fat diet (HCHFD)-induced metabolic syndrome.

Keywords*: Ursolic Acid, Metabolic Syndrome, High-carbohydrate high-fat diet, Vascular oxidative stress, Endothelial dysfunction, Endothelial nitric oxide synthase gene*.

**Authors for correspondence: tosomod2015@gmail.com , Tel: +234-8038580331*

Manuscript received- May 2024; Accepted: September 2024

DOI: https://doi.org/10.54548/njps.v39i2.13

INTRODUCTION

Metabolic syndrome (MS) has become a growing epidemic with over one billion people in the world affected (Tran *et al*., 2020). Obesity is a component of MS. According to recent data, more than 1 billion people in the world are obese, including 650 million adults, 340 million adolescents, and 39 million children, which will cause about 167 million people to become ill by 2025 (WHO, 2022). The components/diagnostic criteria of MS, which are central obesity, elevated blood pressure, impaired glucose tolerance, insulin resistance, and dyslipidemia, are risk factors for the development of cardiovascular disease

(CVD) and type 2 diabetes (T2D) (O'Neill and O'Driscoll, 2015; Tune *et al*., 2017). These risk factors, which are often induced by high-carbohydrate high-fat diet (HCHFD) (Omodara *et al*., 2022) together with sedentary lifestyle, are associated with vascular dysfunction (Tran *et al*., 2020).

The maintenance of normal vascular homeostasis depends essentially on healthy endothelial cell layer. In normal physiology, the endothelium produces several paracrine factors that regulate vascular tone, limit expression of proinflammatory molecules, inhibit platelet aggregation, promote fibrinolysis, and limit smooth muscle proliferation (Meyers and Gokce, 2007; Lee *et al*., 2017). Endothelial-derived nitric oxide (NO) is the principal driver of the vasodilatory process. eNOS is mostly expressed in endothelial cells, it synthesizes NO in a pulsatile manner and its activity is markedly increased when intracellular Ca^{2+} rises. With respect to the regulation of vascular tone, one of the most important physiological stimuli for eNOS activation is the frictional force of the flowing blood exerted on the endothelial cell surface, known as the fluid shear stress (Shaul, 2002; Lam *et al*., 2006). This stimulus does not produce sustained increases in intracellular Ca2+ (Forstermann and Sessa, 2012). When exposed to the increased shear stress, healthy endothelium responds with increased NO production owing to the phosphorylation of eNOS (Corson *et al*., 1996). Once synthesized, NO diffuses to VSMC and induces endothelium-dependent, flow-mediated vasodilatation to accommodate the increased flow (Rapoport *et al*., 1983; Forstermann *et al*., 1986). NO molecules vasodilate the local vascular smooth muscles by stimulating guanylyl cyclase and increasing production of cyclic guanosine monophosphate (cGMP) (Forstermann and Sessa, 2012). In addition to its vasodilatory effects, NO also acts as a potent inhibitor of platelet aggregation and adhesion, interferes with leukocyte adhesion, and inhibits proliferation of vascular smooth muscles (Forstermann and Sessa, 2012; Lee *et al*., 2017). Disruption of these processes results in unhealthy endothelium which leads to vascular dysfunction.

Previous data have shown vascular dysfunction in conduit and small arteries in patients with metabolic syndrome (Schillaci *et al*., 2005; Greenstein *et al*., 2009). Dysfunctional resistance arteries play a key role in the development of hypertension and is mediated, at least in part, by oxidative stress (Schiffrin and Touyz, 2004). In the vascular system, reactive oxygen species (ROS) are produced by different cell types, such as endothelial cells, vascular smooth muscle cells, and inflammatory cells infiltrating the perivascular tissue (Di *et al*., 1999; De Ciuceis *et al*., 2005). NADPH oxidase represents the major source of ROS in the vasculature (Schiffrin, 2008). In addition, the enzyme endothelial NO synthase (eNOS), which normally is "coupled" and produces NO, under some conditions, such as in the presence of excess oxidative stress or decreased tetrahydrobiopterin, is "uncoupled" and generates superoxide (·O2−). This leads to the production of reactive nitrogen species, such as peroxynitrite, as a result of the action of ·O2− on NO. Thus, in the vascular system, oxidative stress from different sources decreases NO bioavailability, thereby promoting endothelial dysfunction, vasoconstriction, remodeling, and enhanced systemic vascular resistance, leading to blood pressure increase (Touyz and Schiffrin, 2004; Schiffrin, 2008).

Markers of oxidative stress have been studied as a means to assess endothelial injury and dysfunction because reduction in NO bioavailability is often due to increased pro-oxidant stress. Glutathiones maintains thiol groups of biomolecules in their reduced state and prevents peroxidation of membrane lipids (Molyneux *et al*., 2002). Similarly, high cysteine levels are indicative of increased oxidative stress. Glutathione is also involved in transportation of NO (Bohlen *et al*., 2009). Previous studies have found associations between increased oxidative stress, measured as lower glutathione and/or higher cysteine levels and flow-mediated dilation (FMD), microvascular vasodilator function, arterial stiffness, and arterial thickness (Ashfaq *et al*., 2008; Dhawan *et al*., 2011; Patel *et al*., 2011; Mkhwanazi *et al*., 2014).

Insulin resistance is marked by hyperinsulinemia and hyperglycemia. Under normal conditions, insulin enhances the vasodilatory action of NO and increases its production, however, display paradoxical vasoconstriction when exposed to high level of insulin. In patients with insulin-dependent diabetes mellitus, the serum insulin concentration is inversely correlated with endothelium-dependent vasodilation (EDV) (Johnstone *et al*., 1993). Furthermore, insulin administration itself impairs endothelial function (Arcaro *et al*., 2002). However, this impairment can be reversed with the administration of antioxidant vitamin C. This suggests that hyperinsulinemia increases oxidative stress in the vasculature (Arcaro *et al*., 2002). Vascular oxidative stress and overproduction of ROS have a deleterious effect on eNOS activity and synthesis of NO. The ROS in insulin-resistant subjects enhance the oxidation of BH4 to 7,8-dihydrobiopterin (BH2), limiting the amount of active cofactor available for eNOS function. The activity of dihydropteridine reductase, an enzyme that regulates the rate of regeneration of BH4 from BH2, is reduced in insulin resistance and compounds on the problem with pteridine metabolism (Shinozaki *et al*., 2001). Finally, ROS directly inactivate NO, thereby decreasing its bioavailability.

Nitric oxide (NO) demonstrates its important role in adipose tissue biology by influencing adipogenesis, insulin-stimulated glucose uptake, and lipolysis. Endothelial nitric oxide synthase (eNOS) is an enzyme responsible for NO formation in adipose cells (Engeli *et al*., 2004). A study by Sansbury *et al*. (2012) demonstrate that increased eNOS activity prevents the obesogenic effects of high-fat diet without affecting systemic insulin resistance thereby stimulating metabolic activity in adipose tissue.

Ursolic acid (UA) is a natural pentacyclic triterpenoid carboxylic acid that is also known as urson, prunol, malol, or 3β-hydroxyurs-12-en-28-oic acid (Mbaveng *et al*., 2014). UA and its related compounds such as oleanolic acid, betulinic acid, uvaol or α- and β-amyrin, are widely distributed in various plants, and have become integral part of human diet (Jager *et al*., 2009; Mbaveng *et al*., 2014). Their content and composition differ between various species, due to the presence and activity of the enzymes responsible for their synthesis. Dietary sources of UA include apple (Malus domestica) fruit; apple peels contain large quantities of ursolic acid and related compounds (Cargnin & Gnoatto, 2017). Several studies, both in vitro and in vivo, have revealed that UA has diverse biological roles, including anti-inflammatory (Kashyap *et al*., 2016), anti-oxidative (Liobikas *et al*., 2011), anti-carcinogenic

(Shishodia *et al*., 2003), anti-obesity (Jayaprakasam *et al*., 2006), and anti-diabetic activities (Kwon *et al*., 2018). We have shown that UA prevents the development of high-carbohydrate high-fat diet (HCHFD)-induced MS (Omodara *et al*., 2022). However, the potential mechanism involved in the amelioration of vascular dysfunction and oxidative stress induced by HCHFD has not been explained. This study investigated the mechanism by which dietary UA supplementation improves vascular oxidative stress in male Wistar rats fed a HCHFD.

MATERIALS AND METHODS

Experimental Animals: A total of twenty (20) male Wistar rats, 8-9 weeks old and weighing 120 - 170 grams were housed in well-aerated plastic cages and allowed to acclimatize having free access to commercial grower mash feed and water ad libitum. After two weeks of acclimatization, the cages' beddings were changed from shaving sawdust to aluminium beddings. This allowed us to quantify spill over food and measure total daily food consumption.

Table 1:
Macronutrients in a normal diet and HCHF diet

Macronutrient	Normal diet	HCHF diet
Total carbohydrate (g/100g)	57.24	53.82
Total fat (g/100g)	4.78	17.29
Protein (g/100g)	25.76	14.05
Crude fibre (g/100g)	2.68	1.44
Ash (g/100g)	5.62	3.40
Moisture (g/100g)	4.06	10.02

Note:
Drinking water in the HCHFD-fed rats was augmented with 20% fructose.

Formulation of High-carbohydrate High-fat Diet (HCHFD):
The high-carbohydrate, high-fat diet (HCHFD) was formulated in-house following the method of Panchal *et al*. (2011) and Wong *et al*. (2017) with little modification. The high-carbohydrate, high-fat diet consists of condensed milk (39.5%), fructose (17.5%), thermally oxidized palm oil (20%), Powdered rat food (15.5%), Hubble, Mendel & Wakeman (HMW) salt mixture (2.5%), and water (5%) together with 20% fructose in drinking water (Omodara *et al*., 2022). Proximate analysis of the diets was carried out by the method of AOAC (2006) and the results are presented in table 1 below.

Preparation of Thermally Oxidized Palm Oil: Fresh palm oil was thermally oxidized as described previously (Osim *et al*., 1992). Briefly, fresh palm oil was subjected to heat at 150°C in a stainless-steel pot. The heating was for five rounds, and each round lasted 20 minutes. After each round, the oil was allowed to cool for 5 hours. The obtained thermally oxidized palm oil was then used in the formulation of the HCHFD.

Experimental Design: After two weeks of acclimatization, animals were randomly divided into 4 groups and treated as follows:

(i) Group 1: Normal diet-fed rats + Distilled water (ND+DW; n = 5),
(ii) Group 2: ND + Ursolic acid (ND+UA; n = 5),
(iii) Group 3: High-carbohydrate high-fat diet-fed rats (HCHFD) + Distilled water (DW) (HCHFD + DW, n = 5),
(iv) Group 4: HCHFD + Ursolic acid (HCHFD+UA, n = 5).

Feeding of Animals and Administration of Ursolic Acid: The animals were fed their respective diets daily for 20 weeks. The ND-fed rats were provided with normal tap water while drinking water in the HCHFD-fed rats was augmented with 20% fructose. A dose of 250 mg/kg body weight of ursolic acid (Zhang *et al*., 2016) was adopted. Ursolic acid was dissolved in an equal volume of distilled water and 50% DMSO, and administered orally through oral gavage to both ND+UA and HCHFD+UA groups starting 12 weeks after initiation of the HCHFD for a further 8 weeks period.

Determination of Percentage Change in Body Mass Index: All rats were monitored daily for food and water intake. The body weight of rats was measured every 4 weeks from week 0 until week 12 and measured weekly from week 12 until week 20 using a standard weighing scale. While body length (nose to anus) and abdominal circumference were measured using a standard measuring tape every 4 weeks. The body mass index (BMI) of each rat was calculated as body weight (in grams) / [body length (in centimeters)]2 (Panchal *et al*., 2011). The difference between BMI values at weeks 0 and 20 were determined and used to calculate the percentage change (increase).

Calculation of Percentage Change or Increase:
Change = values at week 20 – values at week 0.
If the change is positive, it means there is an increase and if negative, it means there is a decrease. In this study, all changes were positive, meaning there were increases. Therefore, in this study, the percentage increase was calculated as follows:
Percentage increase (%) = increase/values at week 0 x 100.

Biochemical Analysis, Animal sacrifice, blood sample collection and tissue processing: At the end of 20 weeks, animals were fasted overnight for 12 hours and anesthetized using a combination of 75 mg/kg body weight of ketamine and 5 mg/kg body weight of diazepam injection, and blood samples were collected via cardiac puncture (Flecknell, 2009). The blood samples, collected in plain bottles, were centrifuged for 10 minutes at 6000RPM to harvest the serum. The serum was collected, stored at -70°C and used for insulin and nitric oxide assay. Descending abdominal aorta and adipose tissues were isolated, washed in phosphate-buffered solution (pH 7.4) and homogenised with phosphate-buffered solution, centrifuged at 447 x g for approximately 20 min. The supernatant was carefully collected and used for the assay of reactive oxygen species, superoxide dismutase, catalase, glutathione and determination of expression levels of eNOS mRNA.

ELISA kits techniques: Insulin ELISA kits, nitric oxide (NO) ELISA kits, reactive oxygen species (ROS) ELISA Kits, Superoxide dismutase (SOD) ELISA kits, catalase

(CAT) ELISA kits and glutathione (GSH) ELISA kits were purchased from Coon Koon Biotech®, Shanghai, China. The assays were done following the manufacturer's manual based on the principles of each of the test. ELISA microplate reader was used to read the absorbance and the concentration of the solutions.

Homeostasis Model Assessment for Insulin Resistance (HOMA-IR): Insulin resistance was determined by the formula:
HOMA-IR = fasting blood glucose (mg/dl) x fasting insulin (µiu/ml)/405 (Matthews *et al*., 1985; Cho *et al*., 2017).

Real-time polymerase chain reaction: The descending abdominal aorta and retroperitoneal adipose tissues were harvested and used to determine the levels of expression of eNOS mRNA by the real-time PCR method. Primer centrifuging was done using a micro refrigerated centrifuge (MTX-150) at 15,000 RPM. The primers were then reconstituted by using 150 µl of PCR graded water. Primer sequences were designed using the National Center for Biotechnology Information Primer Design tool. All primers were purchased from BIONEER, USA. The synthesized sequences of PCR primers are: eNOS – forward: 5′-TATTTGATGCTCGGGACTGC-3′ and reverse: 5′-AAGATTGCCTCGGTTTGTTG-3'. β-actin – forward: 5'-TTGTAACCAACTGGGACGATATGG-3' and reverse: 5'-GATCTTGATCTTGATGGTGCTGCTAGG-3'. β-actin primer was used as a housekeeping gene primer to amplify the endogenous control product (Padilla *et al*., 2014).
RNA extraction was carried out under ice rack. Samples were homogenized with a homogenizer and 500 µl of RB Buffer was added. The lysate was centrifuged at 13,000 RPM for 3 minutes and the supernatant was transferred into a new microcentrifuge tube. 200 µl of 100% ethanol was added and mix immediately using pipette. The sample was then transferred to a binding column in a 2 ml collection tube, the lid was closed and centrifuged at 14,000 RPM for 20 seconds. 700 µl of RWA1 was added without wetting the rim and centrifuged at 14,000 RPM for 20 seconds and supernatant was discarded. The sample was transferred into another collection tube and 500 µl of RWA2 Buffer was added without wetting the rim and centrifuged at 14,000 RPM for 20 seconds and supernatant also discarded. The sample was transferred into another collection tube and 500 µl of RWA2 Buffer was added without wetting the rim and centrifuged at 14,000 RPM for 4 minutes (2 minutes per orientation) and supernatant discarded. Ethanol was completely removed by centrifuging once more at 14,000 RPM for 1 minute. The binding column was then transferred to a new 1.5 ml tube for elusion by adding 50 µl of ER Buffer and after waiting for 5 minutes at room temperature (25oC), we centrifuged at 10,000 RPM for 1 minute to elute. After total RNA extraction, cDNA was synthesized from total RNA using the High-Capacity cDNA Reverse Transcription kit (BIONEER, USA). 3 µl of each primer and 17 µl of each RNA, making 20 µl, were added to each reaction in the reverse transcription premix tube. The tubes were loaded in the PCR machine at 42oC for 1 hour. Quantitative real-time polymerase chain reaction (PCR) was performed using the Real-Time PCR Detection System (Applied Biosystem GeneAmpR). Primers and cDNA were thawed. A 20-µL reaction mixture containing 10-µL of real-time PCR reagent (AccuPowerR 2X GreenStarTM qPCR Master Mix, BIONEER, USA), 4-µL of gene-specific primers (2-µL for forward primer and 2-µL for reverse primer) plus 4-µL of cDNA template, together with appropriate concentration of PCR graded water and ROX dye in PCR tubes. The mixture was mixed by vortexing and the tubes were sealed using optical adhesive film for real-time PCR. Centrifuging was done at 3,000 RPM for 2 minutes and the tubes were loaded into the Real-Time PCR Detection System. The reactions were performed under the following conditions:

Table 2:
PCR conditions

Step	Temperature	Time	Cycles
Pre-denaturation	94 ºC	5 min	1 cycle
Denaturation	94 ºC	30 sec	40
Annealing	54 ºC	30 sec	Cycles
Extension	72 ºC	30 sec	
Final extension	72 ºC	5 min	

Thereafter, mRNA expression level was determined as fold change (FC) as follows:

$$FC = 2^{(-\Delta\Delta Ct)}$$ **(**Livak and Schmittgen, 2001).

Statistical Analysis: Data were expressed as mean ± standard error of the mean (SEM). Data were analyzed using one-way analysis of variance (ANOVA), followed by the Tukey post-hoc test. Values at P<0.05 was considered statistically significant. The SPSS version 23 (IBM, Armonk, NY, USA) was used for statistical analysis.

RESULTS

Effect of ursolic acid on body mass index in male Wistar rats fed a high-carbohydrate high-fat diet: Figure 1 shows that the HCHFD+DW group had a significantly (P<0.05) higher BMI increase (50.0±0.69) compared to the ND+DW group (23.84±0.57). While the HCHFD+UA-fed rats had a significantly (P<0.05) lower BMI increase (34.78±0.30) compared to the HCHFD+DW group (50.0±0.69).

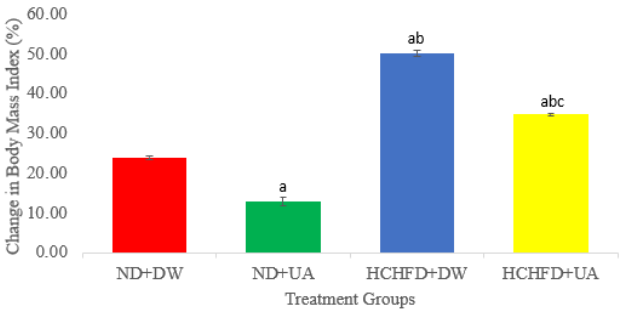

Figure 1:
Percentage change in body mass index in male Wistar rats fed HCHFD and UA. (n = 5 rats per group). UA dose = 250 mg/kg body weight.
Data were expressed as Mean±SEM (n=5). a = significant vs ND+DW at P<0.05; b = significant vs ND+UA at P<0.05; c = significant vs HCHFD+DW at P<0.05. ND+DW: normal diet + distilled water group; ND+UA: normal diet + ursolic acid group; HCHFD+DW: high-carbohydrate high-fat diet + distilled water group; HCHFD+UA: high-carbohydrate high-fat diet + ursolic acid group.

Effect of ursolic acid on fasting serum insulin in male Wistar rats fed a high-carbohydrate high-fat diet: Figure 2 shows that there was a significant increase (P<0.05) in fasting insulin level in the HCHFD+DW group (123.76±0.95) compared to the ND+DW group (73.84±0.72). The HCHFD+UA-fed animals had a significantly lower (P<0.05) insulin level (95.64±0.48) compared to the HCHFD+DW group (123.76±0.95).

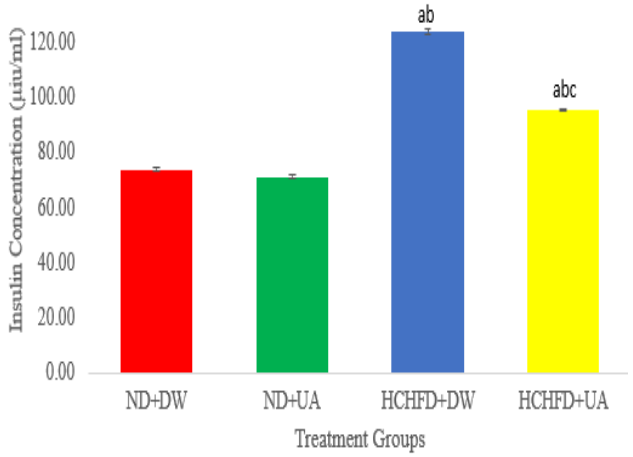

Figure 2:
Serum insulin concentration in male Wistar rats fed HCHFD and UA. (n = 5 rats per group). UA dose = 250 mg/kg body weight. *Data were expressed as Mean±SEM (n=5). a = significant vs ND+DW at P<0.05; b = significant vs ND+UA at P<0.05; c = significant vs HCHFD+DW at P<0.05. ND+DW: normal diet + distilled water group; ND+UA: normal diet + ursolic acid group; HCHFD+DW: high-carbohydrate high-fat diet + distilled water group; HCHFD+UA: high-carbohydrate high-fat diet + ursolic acid group*

Effect of ursolic acid on homeostatic model assessment for insulin resistance in male Wistar rats fed a high-carbohydrate high-fat diet: Figure 3 shows that there was a significant increase (P<0.05) in HOMA-IR level in the HCHFD+DW group (36.72±0.53) compared to the ND+DW group (16.70±0.34). The HCHFD+UA-fed animals had a significantly lower (P<0.05) HOMA-IR level (23.0±0.34) compared to the HCHFD+DW group (36.72±0.53).

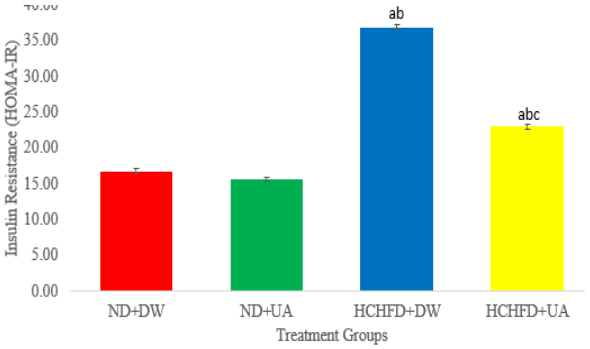

Figure 3:
Homeostatic model assessment for insulin resistance in male Wistar rats fed HCHFD and UA. (n = 5 rats per group). UA dose = 250 mg/kg body weight. *Data were expressed as Mean±SEM (n=5). a = significant vs ND+DW at P<0.05; b = significant vs ND+UA at P<0.05; c = significant vs HCHFD+DW at P<0.05. ND+DW: normal diet + distilled water group; ND+UA: normal diet + ursolic acid group; HCHFD+DW: high-carbohydrate high-fat diet + distilled water group; HCHFD+UA: high-carbohydrate high-fat diet + ursolic acid group.*

Effect of ursolic acid on aorta superoxide dismutase in male Wistar rats fed a high-carbohydrate high-fat diet: Figure 4 shows that there was a significant decrease (P<0.05) in the level of aorta SOD in the HCHFD+DW group (28.82±1.02) compared to the ND+DW group (48.68±1.10). The HCHFD+UA-fed animals had a significantly higher (P<0.05) level of aorta SOD (49.34±1.14) compared to the HCHFD+DW group (28.82±1.02).

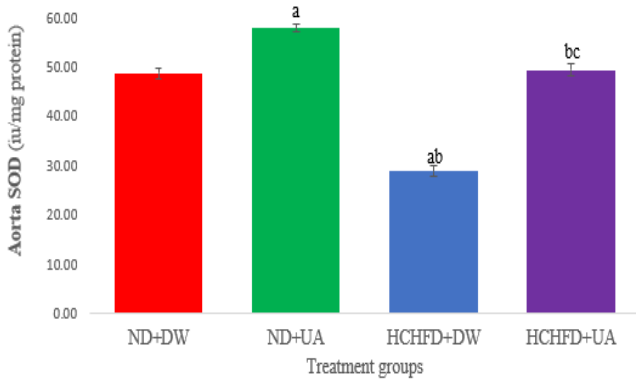

Figure 4:
Levels of aorta superoxide dismutase in male Wistar rats fed HCHFD and UA. (n = 5 rats per group). UA dose = 250 mg/kg body weight**.** *Data were expressed as Mean±SEM (n=5). a = significant vs ND+DW at P<0.05; b = significant vs ND+UA at P<0.05; c = significant vs HCHFD+DW at P<0.05. ND+DW: normal diet + distilled water group; ND+UA: normal diet + ursolic acid group; HCHFD+DW: high-carbohydrate high-fat diet + distilled water group; HCHFD+UA: high-carbohydrate high-fat diet + ursolic acid group.*

Effect of ursolic acid on aorta catalase in male Wistar rats fed a high-carbohydrate high-fat diet: Figure 5 shows that there was a significant decrease (P<0.05) in the level of aorta catalase in the HCHFD+DW group (39.50±1.50) compared to the ND+DW group (53.32±2.09). The HCHFD+UA-fed animals had a significantly higher (P<0.05) level of aorta catalase (57.84±1.50) compared to the HCHFD+DW group (39.50±1.50).

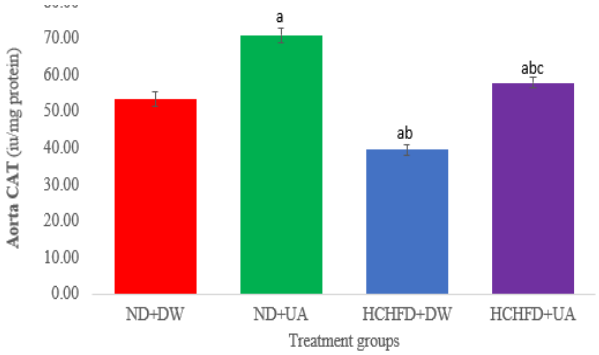

Figure 5:
Levels of aorta catalase in male Wistar rats fed HCHFD and UA. (n = 5 rats per group). UA dose = 250 mg/kg body weight**.**
Data were expressed as Mean±SEM (n=5). a = significant vs ND+DW at P<0.05; b = significant vs ND+UA at P<0.05; c = significant vs HCHFD+DW at P<0.05. ND+DW: normal diet + distilled water group; ND+UA: normal diet + ursolic acid group; HCHFD+DW: high-carbohydrate high-fat diet + distilled water group; HCHFD+UA: high-carbohydrate high-fat diet + ursolic acid group.

Effect of ursolic acid on aorta glutathione in male Wistar rats fed a high-carbohydrate high-fat diet: Figure 6 shows that there was a significant decrease (P<0.05) in the level of aorta glutathione in the HCHFD+DW group (9.76±0.19) compared to the ND+DW group (14.58±0.41). The HCHFD+UA-fed animals had a significantly higher (P<0.05) level of aorta glutathione (13.58±0.42) compared to the HCHFD+DW group (9.76±0.19).

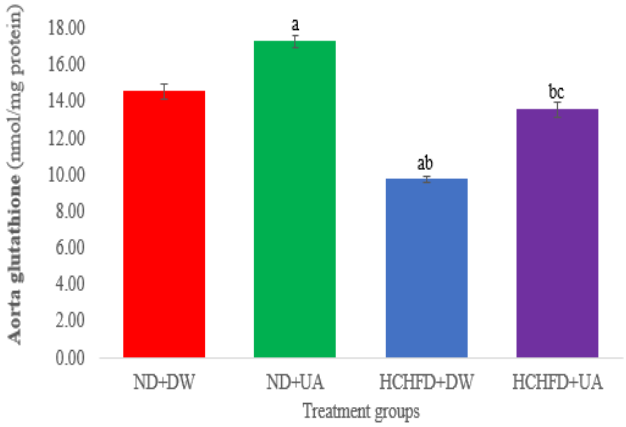

Figure 6:
Levels of aorta glutathione in male Wistar rats fed HCHFD and UA. (n = 5 rats per group). UA dose = 250 mg/kg body weight.
Data were expressed as Mean±SEM (n=5). a = significant vs ND+DW at P<0.05; b = significant vs ND+UA at P<0.05; c = significant vs HCHFD+DW at P<0.05. ND+DW: normal diet + distilled water group; ND+UA: normal diet + ursolic acid group; HCHFD+DW: high-carbohydrate high-fat diet + distilled water group; HCHFD+UA: high-carbohydrate high-fat diet + ursolic acid group.

Effect of ursolic acid on serum nitric oxide in male Wistar rats fed a high-carbohydrate high-fat diet: Figure 7 shows that level of serum NO significantly decreased (P<0.05) in the HCHFD+DW group (24.30±1.01) compared to the ND+DW group (28.50±0.96). There was a significant increase (P<0.05) in the level of serum NO in the HCHFD+UA-fed animals (38.96±0.97) compared to the HCHFD+DW group (24.30±1.01).

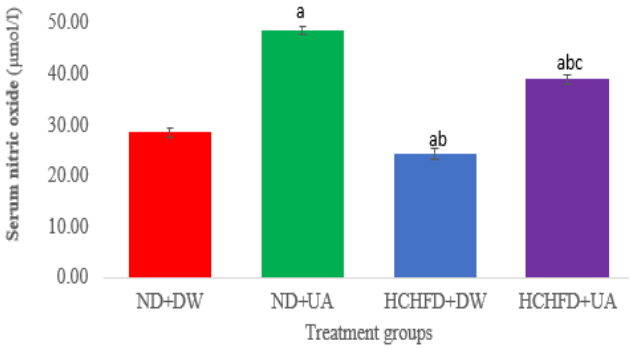

Figure 7:
Levels of serum nitric oxide in male Wistar rats fed HCHFD and UA. (n = 5 rats per group). UA dose = 250 mg/kg body weight.
Data were expressed as Mean±SEM (n=5). a = significant vs ND+DW at P<0.05; b = significant vs ND+UA at P<0.05; c = significant vs HCHFD+DW at P<0.05. ND+DW: normal diet + distilled water group; ND+UA: normal diet + ursolic acid group; HCHFD+DW: high-carbohydrate high-fat diet + distilled water group; HCHFD+UA: high-carbohydrate high-fat diet + ursolic acid group.

Effect of ursolic acid on aorta reactive oxygen species in male Wistar rats fed a high-carbohydrate high-fat diet: Figure 8 shows that level of aorta ROS significantly increased (P<0.05) in the HCHFD+DW group (521.76±0.84) compared to the ND+DW group (259.02±0.44). There was a significant decrease (P<0.05) in the level of aorta ROS in the HCHFD+UA-fed animals (331.00±0.52) compared to the HCHFD+DW group (521.76±0.84).

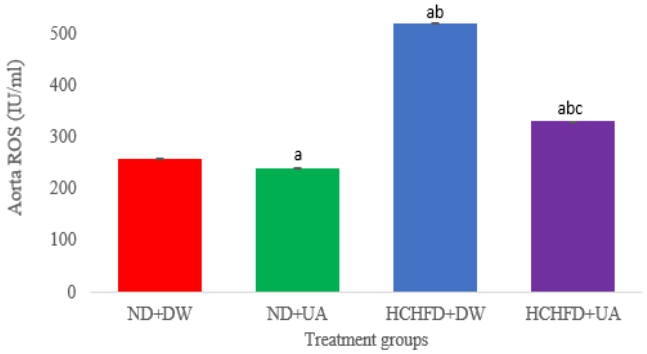

Figure 8:
Levels of serum nitric oxide in male Wistar rats fed HCHFD and UA. (n = 5 rats per group). UA dose = 250 mg/kg body weight**.**
Data were expressed as Mean±SEM (n=5). a = significant vs ND+DW at P<0.05; b = significant vs ND+UA at P<0.05; c = significant vs HCHFD+DW at P<0.05. ND+DW: normal diet + distilled water group; ND+UA: normal diet + ursolic acid group; HCHFD+DW: high-carbohydrate high-fat diet + distilled water group; HCHFD+UA: high-carbohydrate high-fat diet + ursolic acid group.

Effect of ursolic acid on aorta eNOS mRNA expression in male Wistar rats fed a high-carbohydrate high-fat diet. Figure 9 shows that aortic eNOS mRNA level was significantly (P<0.05) downregulated in the HCHFD+DW-fed rats (0.26±0.06) compared to normal control (1.00±0.04). Treatment with UA significantly (P<0.05) upregulated aortic eNOS mRNA level in the HCHFD+UA-fed rats (0.92±0.03) compared to the HCHFD+DW-fed rats (0.26±0.06).

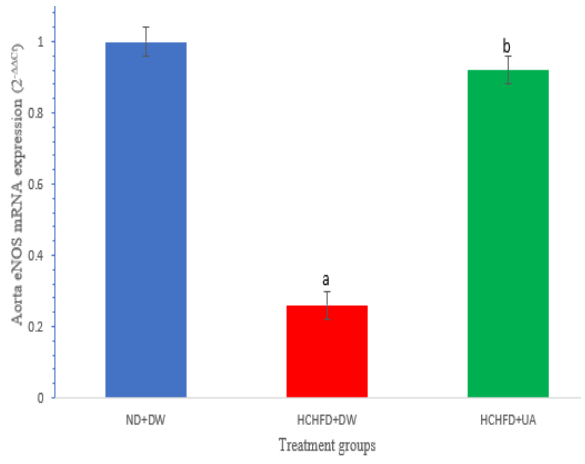

Figure 9:
Aortic eNOS mRNA expression in HCHFD and ursolic acid-treated male Wistar rats. (n = 5 rats per group). UA dose = 250 mg/kg body weight.
ND+DW: normal diet + distilled water group; HCHFD+DW: high-carbohydrate high-fat diet + distilled water group; HCHFD+UA: high-carbohydrate high-fat diet + ursolic acid group.
a = significant vs ND+DW; b = significant vs HCHFD+DW, at P<0.05

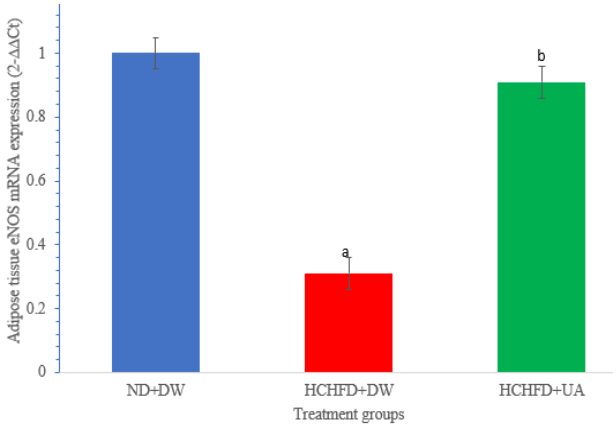

Figure 10:
Adipose tissue eNOS mRNA expression in HCHFD and ursolic acid-treated male Wistar rats. (n = 5 rats per group). UA dose = 250 mg/kg body.
ND+DW: normal diet + distilled water group; HCHFD+DW: high-carbohydrate high-fat diet + distilled water group; HCHFD+UA: high-carbohydrate high-fat diet + ursolic acid group.
a = significant vs ND+DW; b = significant vs HCHFD+DW, at P<0.05

Effect of ursolic acid on adipose tissue eNOS mRNA expression in male Wistar rats fed a high-carbohydrate high-fat diet: Figure 10 shows that adipose tissue eNOS mRNA level was significantly (P<0.05) downregulated in the HCHFD+DW-fed rats (0.31±0.04) compared to normal control (1.00±0.05). Treatment with UA significantly (P<0.05) upregulated adipose tissue eNOS mRNA level in the HCHFD+UA- fed rats (0.91±0.06) compared to HCHFD+DW-fed rats (0.31±0.04).

DISCUSSION

The results of this study did not only demonstrate metabolic syndrome-related HCHFD-induced vascular oxidative stress, but also showed that ursolic acid has the potential to ameliorate this effect.
The results of this study showed that HCHFD increased body mass index (BMI). BMI is a marker of obesity (Novelli *et al*., 2007). According to Lobato *et al*. (2012), the severity of vascular endothelial dysfunction strongly correlates with the degree of visceral adiposity, probably due to adipocyte hypertrophy. Also, 20 weeks of feeding on HCHFD increased serum insulin and HOMA-IR. The increased HOMA-IR, which is as a result of increased fasting blood glucose and serum insulin, suggests insulin resistance. High fat feeding in mice has been shown to induce insulin resistance. (Zabolotny *et al*., 2008; Agouni *et al*., 2011). Insulin resistance has been linked to vascular dysfunction (Eringa *et al*., 2007).

The findings from this study showed that HCHFD significantly decreased aorta antioxidant enzymes (SOD, CAT and GSH). This finding suggests increased vascular oxidative stress (Panchal *et al*., 2011). This study also showed that HCHFD significantly increased levels of aorta reactive oxygen species (ROS). Fructose feeding is associated with the induction of oxidative stress (Stanhope & Havel, 2008). An imbalance between the production of ROS and the ability of the antioxidant systems to readily detoxify these reactive intermediates results in oxidative stress (Stanhope & Havel, 2008). Significant increase in aortic free radicals combined with decreased aortic antioxidant defense systems is an indication of vascular oxidative stress. Free radicals generated in excessive and uncontrollable amounts under oxidative stress conditions cause damage to DNA, proteins, and lipids, which can severely compromise cell health and contribute to disease development (Birben *et al*., 2012).

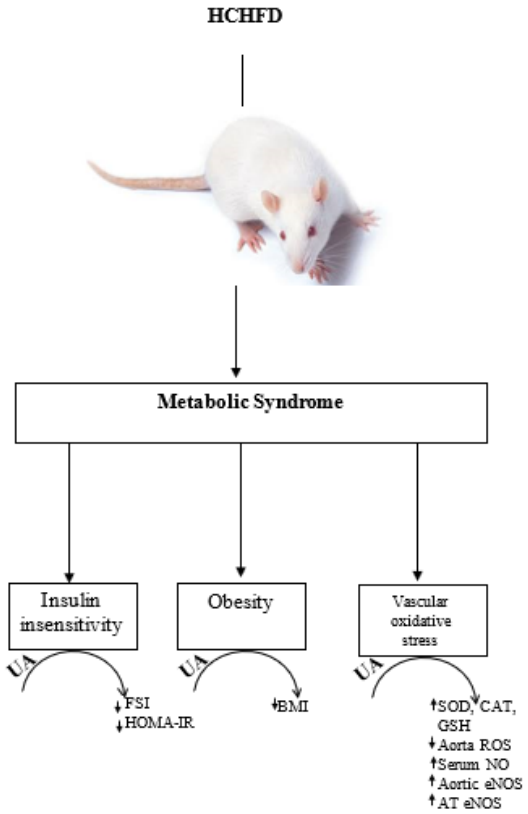

↓ = Decrease, ↑ = Increase. FSI – fasting serum insulin, HOMA-IR – homeostatic assessment for insulin resistance, BMI – body mass index, SOD – superoxide dismutase, CAT – catalase, GSH – glutathione, ROS – reactive oxygen species, NO – nitric oxide, AT – adipose tissue, eNOS – endothelial nitric oxide synthase, UA – ursolic acid, HCHFD – high-carbohydrate high-fat diet

Figure 11:
Proposed mechanism by which ursolic acid ameliorate metabolic syndrome-related HCHFD-induced vascular dysfunction
.

Results from this study also showed that HCHFD significantly decreased serum nitric oxide (NO) levels, as well as aortic and adipose tissue eNOS mRNA levels. This corroborate the findings of previous studies where they reported that serum NO was reduced (Panchal *et al*., 2011) and eNOS was downregulated (Sansbury and Hill, 2015) in obese rats. Reduced bioavailability of NO is commonly attributed to downregulation of eNOS (Sansbury and Hill, 2015). Inflammatory state occurring in metabolic syndrome has been linked to vascular dysfunction. The cytokine, TNF-α, which is implicated in the initiation of insulin resistance, downregulates eNOS abundance by decreasing the stability of eNOS mRNA (Sansbury and Hill, 2015). Vascular endothelial dysfunction is not only a consequence of insulin

resistance, but also impairs insulin signaling to further reduce insulin sensitivity, thereby resulting in a destructive cycle in metabolic syndrome and diabetes. In obese rats, altered insulin signaling disrupts insulin-mediated NO production via downregulation of eNOS expression to impair vasodilatation in resistance arteries. The involvement of ROS and subsequent degradation of BH4 (a cofactor essential for NO synthesis from eNOS) in insulin resistance is thought to play a role in the impairment of NO-dependent vasodilatation (Eringa *et al*., 2007; Trans *et al*., 2020).

As shown in figure 11, in this present study, obesity, fasting hyperinsulinemia, insulin resistance and vascular oxidative stress, all induced by a 20-weeks feeding on HCHFD were significantly alleviated by UA. Zhang *et al*. (2016) and Ramirez-Rodriquez *et al*. (2017) have reported that the anti-obesity effect of UA occurs possibly via increased Akt phosphorylation and improved skeletal muscle glucose uptake. In this study, the decreased serum insulin and amelioration of insulin resistance by UA suggests that UA may have an insulin sensitizing effect.

The findings of this study also showed that UA significantly increased vascular antioxidant enzymes. This corroborate the findings of Mason *et al*. (2020) and may suggest an enhancement of the antioxidant defense system. In this present study, UA significantly decreased aortic ROS level. This is consistent with the findings of Saad *et al*. (2015) and Pordanjani *et al*. (2022).

Findings from this study showed that UA mitigates vascular oxidative stress through its antioxidative actions demonstrated by decreased aortic free radicals which were probably scavenged by the enhanced antioxidant defense systems.

Also, UA may have the potential to enhance endothelium-derived vasorelaxation (EDVR) due to its ability to significantly increase serum NO levels, as well as aortic and AT eNOS mRNA. The restoration of insulin sensitizing effect by UA as earlier observed, may have synergistic effect with NO to increase the vascular antioxidant defense systems and consequently improve EDVR.

In conclusion, findings from this study demonstrated that 20 weeks of feeding on HCHFD successfully induced metabolic syndrome with features such as obesity, insulin resistance, oxidative stress and impaired vasorelaxation in aortic vasculature of male Wistar rats. However, 8 weeks supplementation with UA ameliorated metabolic syndrome-related insulin insensitivity and oxidative stress in aortic vasculature of HCHFD-fed male Wistar rats and upregulates both aortic and adipose tissue eNOS mRNA. Therefore, it was concluded that UA ameliorates vascular oxidative stress and upregulates eNOS gene in male Wistar rats with HCHFD-induced metabolic syndrome.

Further studies, including vascular reactivity and protein expression studies in aortic vasculature, are recommended.

REFERENCES

Agouni, A. M., Ody, N., Owen, C. (2011). Liver-specific deletion of protein tyrosine phosphatase (PTP) 1B improves obesity- and pharmacologically-induced endoplasmic reticulum stress. *Biochemistry Journal*, 438 (2), 369-378.

AOAC (Association of Official Analytical Chemists), (2006). Official Method of Analysis of the AOAC (W. Horwitz Editor) Eighteenth Edition. Washington D.C, AOAC.

Arcaro, G., Cretti, A., Balzano, S., Lechi, A., Muggeo, M., Bonora, E., Bonadonna, R. C. (2002). Insulin causes endothelial dysfunction in humans: sites and mechanisms. *Circulation*, 105(5), 576-582.

Ashfaq, S., Abramson, J. L., Jones, D. P., Rhodes, S. D., Weintraub, W. S., Hooper, W. C., Alexander, R. W., Vaccarino, V., Harrison, D. G., Quyyumi, A. A. (2008). Endothelial function and aminothiol biomarkers of oxidative stress in healthy adults. *Hypertension*, 52(1), 80-85.

Birben, E., Sahiner, U. M., Sackesen, C., Erzurum, S., Kalayci, O. (2012). "Oxidative stress and antioxidant defense," *The World Allergy Organization Journal*, 5 (1), 9–19.

Bohlen, H. G., Zhou, X., Unthank, J. L., Miller, S. J., Bills, R. (2009). Transfer of nitric oxide by blood from upstream to downstream resistance vessels causes microvascular dilation. *American Journal of Physiology- Heart and Circulatory Physiology*, 297(4), H1337-H1346.

Cargnin, S. T., Gnoatto, S. B. (2017). "Ursolic acid from apple pomace and traditional plants: A valuable triterpenoid with functional properties". Food Chemistry, 220, 477–489.

Cho, J., Hong, H., Park, S., Kim, S., Kang, H. (2017). Insulin resistance and its association with metabolic syndrome in Korean Children. *Biomedical Research International* 2017: 8728017.

Corson, M. A., James, N. L., Latta, S. E., Nerem, R. M., Berk, B. C., Harrison, D. G. (1996). Phosphorylation of endothelial nitric oxide synthase in response to fluid shear stress. *Circulation Research*, 79(5), 984–991.

De Ciuceis, C., Amiri, F., Brassard, P., Endemann, D. H., Touyz, R. M., Schiffrin, E. L. (2005). Reduced vascular remodeling, endothelial dysfunction, and oxidative stress in resistance arteries of angiotensin II-infused macrophage colony-stimulating factor-deficient mice: evidence for a role in inflammation in angiotensin-induced vascular injury. *Arteriosclerosis, Thrombosis and Vascular Biology*, 25, 2106–2113.

Dhawan, S. S., Eshtehardi, P., McDaniel, M. C., Fike, L. V., Jones, D. P., Quyyumi, A. A., Samady, H. (2011). The role of plasma aminothiols in the prediction of coronary microvascular dysfunction and plaque vulnerability. *Atherosclerosis*, 219(1), 266-272.

Di, W. H., Hope, S., Du, Y., Quinn, M. T., Cayatte, A., Pagano, P. J., Cohen, R. A. (1999). Paracrine role of adventitial superoxide anion in mediating spontaneous tone of the isolated rat aorta in angiotensin II-induced hypertension. *Hypertension*, 33, 1225–1232.

Engeli, S., Janke, J., Gorzelniak, K., Bohnke, J., Ghose, N., Lindschau, C., Luft, F. C., Sharma, A. M. (2004). Regulation of the nitric oxide system in human adipose tissue. *Journal of Lipid Research*, 45 (9): 1640-1648.

Eringa, E. C., Stehouwer, C. D., Roos, M. H., Westerhof, N., Sipkema, P. (2007). Selective resistance to vasoactive effects of insulin in muscle resistance arteries of obese Zucker (fa/fa) rats. *Am. J. Physiol. Endocrinol. Metab*. 293 (5), 1134–1139. 10.1152/ajpendo.00516.2006.

Flecknell, P. (2009). Laboratory animal anaesthesia. Elsevier Inc; 3rd edition, 181-190.

Forstermann, U., Sessa, W. C. (2012). Nitric oxide synthases: regulation and function. *European Heart Journal*, 33(7), 829-837, 837a-837d.

Förstermann, U., Mülsch, A., Böhme, E., Busse, R. (1986). Stimulation of soluble guanylate cyclase by an acetylcholine-induced endothelium-derived factor from

rabbit and canine arteries. Circulation Research, 58(4), 531–538.

Greenstein, A. S., Khavandi, K., Withers, S. B., Sonoyama, K., Clancy, O., Jeziorska, M., Laing, I., Yates, A. P., Pemberton, P. W., Malik, R. A., Heagerty, A. M. (2009). Local inflammation and hypoxia abolish the protective anticontractile properties of perivascular fat in obese patients. Circulation, 119, 1661–1670.

Jager, S., Trojan, H., Kopp, T., Laszczyk, M. N., Scheffler, A. (2009). Pentacyclic triterpene distribution in various plants - rich sources for a new group of multi-potent plant extracts. Molecules, 14, 2016–2031.

Jayaprakasam, B., Olson, L. K., Schutzki, R. E., Tai, M. H., Nair, M. G. (2006). Amelioration of obesity and glucose intolerance in high-fat-fed C57BL/6 mice by anthocyanins and ursolic acid in Cornelian cherry (Cornus mas). Journal of Agricultural and Food Chemistry, 54: 243–248.

Johnstone, M. T., Creager, S. J., Scales, K. M., Cusco, J. A., Lee, B. K., Creager, M. A. (1993). Impaired endothelium-dependent vasodilation in patients with insulin-dependent diabetes mellitus. Circulation, 88(6), 2510-2516.

Kashyap, D., Sharma, A., Tuli, H. S., Punia, S., Sharma, A. K. (2016). Ursolic acid and oleanolic acid: pentacyclic terpenoids with promising antiinflammatory activities. Recent Patents on Inflammation & Allergy Drug Discovery, 10: 21–33.

Klatt, P., Pfeiffer, S., List, B. M. (1996). Characterization of heme-deficient neuronal nitric-oxide synthase reveals a role for heme in subunit dimerization and binding of the amino acid substrate and tetrahydrobiopterin. *Journal of Biological Chemistry*, 271(13), 7336–7342.

Kwon, E. Y., Shin, S. K., Choi, M. S. (2018). Ursolic Acid Attenuates Hepatic Steatosis, Fibrosis, and Insulin Resistance by Modulating the Circadian Rhythm Pathway in Diet-Induced Obese Mice. *Nutrients*, 10: 1-15.

Lam, C. F., Peterson, T. E., Richardson, D. M. (2006). Increased blood flow causes coordinated upregulation of arterial eNOS and biosynthesis of tetrahydrobiopterin. *American Journal of Physiology* – Heart and Circulatory Physiology, 290(2), H786–H793.

Lee, S. K., Khambhati, J., Bhargava, A., Engels, M. C., Sandesara, P. B., Quyyumi, A. A. (2017). Endothelial Dysfunction and Metabolic Syndrome. *Hypertension Journal*, 3(2), 72-80.

Liobikas, J., Majiene, D., Trumbeckaite, S., Kursvietiene, L., Masteikova, R., Kopustinskiene, D. M., Savickas, A., Bernatoniene, J. (2011). Uncoupling and antioxidant effects of ursolic acid in isolated rat heart mitochondria. *Journal of Natural Product*, 74: 1640–1644.

Livak, K. J, Schmittgen, T. D. (2001). Analysis of relative gene expression data using real-time quantitative PCR and the 2(-Delta Delta C(T)) Method. Methods San Diego Calif 25:402–8.

Mason, S. A., Trewin, A. J., Parker, L., Wadley, G. D. (2020). Antioxidant supplements and endurance exercise: Current evidence and mechanistic insights. *Redox Biology*; 35: 101471.

Matthews, D. R., Hosker, J. P., Rudenski, A. S., Naylor, B. A., Treacher, D. F., Turner, R. C. (1985). Homeostasis model assessment:insulin resistance and beta-cell function from fasting plasma glucose and insulin concentrations in man. *Diabetologia* 28: 412–19.

Mbaveng, A. T., Hamm, R., Kuete, V. (2014). Harmful and Protective Effects of Terpenoids from African Medicinal Plants. Toxicological Survey of African Medicinal Plants, *Elsevier Inc*; 557-576, ISBN: 9780128000182.

Meyers, M. R., Gokce, N. (2007). Endothelial dysfunction in obesity: etiological role in atherosclerosis. *Current opinion of endocrinology, diabetes and obesity.* 14(5), 365-369.

Mkhwanazi, B. N., Serumula, M. R., Myburg, R. B., Van Heerden, F. R., Musabayane, C. T. (2014). Antioxidant effect of maslinic acid in livers, hearts and kidneys of streptozotocin-induced diabetic rats: effects on kidney function. *Renal failure*, 36(3), 419-431.

Molyneaux, C. A., Glyn, M. C., Ward, B. J. (2002). Oxidative stress and cardiac microvascular structure in ischemia and reperfusion: the protective effect of antioxidant vitamins. *Microvascular research*, 64(2), 265-277.

Novelli, E. L., Diniz, Y. S., Galhardi, C. M., Ebaid, G. M., Rodrigues, H. G., Mani, F., Fernandes, A. A., Cicogna, A. C., Novelli Filho, J. L. (2007). Anthropometrical parameters and markers of obesity in rats. *Laboratory Animals* 41(1): 111-9.

O'Neill, S., O'Driscoll, L. (2015). Metabolic syndrome: a closer look at the growing epidemic and its associated pathologies. *Obes Rev*.; 16 (1), 1–12. 10.1111/obr.12229.

Omodara, O. O., Kawu, M. U., Bako, I. G. (2022). Ursolic acid prevents the development of metabolic syndrome in male Wistar rats fed a high-carbohydrate high-fat diet. *Journal of African Association of Physiological Sciences*, 10(1): 1-12.

Osim, E. E., Owu, D. U., Isong, E. U., Umoh, I. B. (1992). Influence of chronic consumption of thermoxidized palm oil diet on platelet aggregation in rat. *Discovery and Innovation*, 4: 83087.

Padilla, J., Jenkins, N. T., Thorne, P. K., Lansford, K. A., Fleming, N. J., Bayless, D. S., Sheldon, R. D., Rector, R. S., Laughlin, M. H. (2014). Differential regulation of adipose tissue and vascular inflammatory gene expression by chronic systemic inhibition of NOS in lean and obese rats. *Physiological Reports* 2(2): 1-16.

Panchal, S. K., Poudyal, H., Iyer, A., Nazer, R., Alam, M., Diwan, V., Kauter, K., Sernia, C., Campbell, F., Ward, L., Gobe, G., Fenning, A., Brown, L. (2011). High-carbohydrate, High-fat Diet–induced Metabolic Syndrome and Cardiovascular Remodeling in Rats. *Journal of Cardiovascular Pharmacology*, 57: 611–624.

Patel, R. S., Al Mheid, I., Morris, A. A., Ahmed, Y., Kavtaradze, N., Ali, S., Uphoff, I., Sher, S., Dabhadkar, K., Aznaouridis, K. (2011). The oxidized aminothiol cysteine is associated with impaired arterial indices in healthy human subjects. *Atherosclerosis*, 218(1), 90-95.

Pordanjani, M. K., Banitalebi, E., Roghani, M., Hemmati, R. (2022). Ursolic acid enhances training on vascular aging by reducing oxidative stress in aged type 2 diabetic rats. *Food Sciences & Nutrition;* 11(2): 696-708; https://doi.org/10.1002/fsn3.3105.

Ramírez-Rodríguez, A. M., González-Ortiz, M., Martínez-Abundis, E., Acuña Ortega, N. (2017). Effect of ursolic acid on metabolic syndrome, insulin sensitivity, and inflammation. *Journal of Medicinal Food* 20: 882–886.

Rapoport, R. M., Draznin, M. B., Murad, F. (1983). Endothelium-dependent relaxation in rat aorta may be mediated through cyclic GMP-dependent protein phosphorylation. Nature, 306(5949), 174–176.

Saad, E. A., Hassanien, M. M., El-Hagrasy, M. A., Radwan, K. H. (2015). Antidiabetic, hypolipidemic and antioxidant activities and protective effects of Punica granatum peels powder against pancreatic and hepatic tissues injuries in streptozotocin-induced IDDM in rats. *International Journal of Pharmacy and Pharmaceutical Sciences*; 7(7): 397-402.

Sansbury, B. E., Cummins, T. D., Tang, Y., Hellmann, J., Holden, C. R., Harbeson, M. A., Chen, Y., Patel, R. P., Spite, M., Bhatnagar, A., Hill, B. G. (2012). Overexpression of

endothelial nitric oxide synthase prevents diet-induced obesity and regulates adipocyte phenotype. *Circulation Research*, 111: 1176-1189.

Sansbury, B. E., Hill, B. G. (2015). Anti-obesogenic role of endothelial nitric oxide synthase. Vitamins and Hormones, 96, 323-346.

Schiffrin, E. L., Touyz, R. M. (2004). From bedside to bench to bedside: role of renin-angiotensin-aldosterone system in remodeling of resistance arteries in hypertension. American *Journal of Physiology – Heart and Circulatory Physiology*, 287, H435–H446.

Schiffrin, E. L. (2008). Oxidative stress, nitric oxide synthase, and superoxide dismutase: a matter of imbalance underlies endothelial dysfunction in the human coronary circulation. *Hypertension*, 51, 31–32.

Schillaci, G., Pirro, M., Vaudo, G., Mannarino, M. R., Savarese, G., Pucci, G., Franklin, S. S., Mannarino, E. (2005). Metabolic syndrome is associated with aortic stiffness in untreated essential hypertension. *Hypertension*, 45, 1078–1082.

Shaul, P. W. (2002). Regulation of endothelial nitric oxide synthase: location, location, location. *Annual Review of Physiology*, 64, 749–774.

Shinozaki, K., Hirayama, A., Nishio, Y., Yoshida, Y., Ohtani, T., Okamura, T., Masada, M., Kikkawa, R., Kodama, K., Kashiwagi, A. (2001). Coronary endothelial dysfunction in the insulin-resistant state is linked to abnormal pteridine metabolism and vascular oxidative stress. *Journal of American College of Cardiology*, 38(7), 1821-1828.

Shishodia, S., Majumdar, S., Banerjee, S., Aggarwal, B. B. (2003). Ursolic acid inhibits nuclear factor-kappaB activation induced by carcinogenic agents through suppression of IkappaBalpha kinase and p65 phosphorylation: correlation with down-regulation of cyclooxygenase 2, matrix metalloproteinase 9, and cyclin D1. *Cancer Research*, 63: 4375–4383.

Stanhope, K. L., Havel, P. J. (2008). Fructose consumption: potential mechanisms for its effects to increase visceral adiposity and induce dyslipidemia and insulin resistance. *Current Opinion in Lipidology, 19, 16–24.*

Tran, V., De Silva, T. M., Sobey, C. G., Lim, K., Drummond, G. R., Vinh, A., Jelinic, M. (2020). The vascular consequences of metabolic syndrome: Rodent models, endothelial dysfunction, and current therapy. *Front Pharmacol*.; 11: 148. doi: 10.3389/fphar.2020.00148.

Tune, J. D., Goodwill, A. G., Sassoon, D. J., Mather, K. J. (2017). Cardiovascular consequences of metabolic syndrome. Transl. Res.; 183, 57–70. 10.1016/j.trsl.2017.01.001.

Wong, S. K., Chin, K. Y., Suhaimi, F. H., Ahmad, F., Ima-Nirwana, S. (2017) The Effects of a Modified High-carbohydrate High-fat Diet on Metabolic Syndrome Parameters in Male Rats. *Experimental and Clinical Endocrinology and Diabetes*, DOI https://doi.org/10.1055/s-0043-119352.

World Health Organization (2022). World Obesity Day 2022 – Accelerating action to stop obesity. Available online: https://www.who.int/news/item/04-03-2022-world-obesity-day-2022-accelerating-action-to-stop-obesity (accessed on 8 August 2022).

Zabolotny, J. M., Kim, Y. B., Welsh, L. A., Kershaw, E. E., Neel, B. G., Khan, B. B. (2008). Protein-tyrosine phosphatase 1B expression is induced by inflammation in vivo. *Journal of Biological Chemistry*, 283 (21), 14230-14241.

Zhang, Y., Song, C., Li, H., Hou, J., Li, D. (2016). Ursolic acid prevents augmented peripheral inflammation and inflammatory hyperalgesia in high-fat diet-induced obese rats by restoring downregulated spinal PPARα. *Molecular Medicine Reports*, 13: 5309-5316.

Zhang, Y., Song, C., Li, H., Hou, J., Li, D. (2016). Ursolic acid prevents augmented peripheral inflammation and inflammatory hyperalgesia in high-fat diet-induced obese rats by restoring downregulated spinal PPARα. *Molecular Medicine Reports*, 13: 5309-5316..